ELSEVIER

Journal of Nuclear Materials 241–243 (1997) 684–689

journal of nuclear materials

Study of gross and net erosion in the ASDEX Upgrade divertor

K. Krieger [a,*], J. Roth [a], A. Annen [a], W. Jacob [a], C.S. Pitcher [a,b], W. Schneider [a], A. Thoma [a], M. Weinlich [a], ASDEX Upgrade Team [a]

[a] *Max-Planck-Institut für Plasmaphysik, EURATOM-Association, 85748 Garching, Germany*
[b] *CFFTP, Toronto, Canada*

Abstract

Erosion of carbon and tungsten in the divertor of ASDEX Upgrade was investigated by surface analysis of target tile probes. The probes were exposed in the divertor using a manipulator system. Erosion of carbon was measured by graphite probes covered with a 150 nm layer of ^{13}C isotope to distinguish from the intrinsic carbon content. Tungsten erosion was measured by similar probes with 1–20 nm tungsten markers evaporated on the surface. From the measured erosion, sputtering yields were determined using plasma parameters at the target plates obtained from flush mounted Langmuir probes.

Keywords: ASDEX Upgrade; Erosion and particle deposition diagnostic; Low Z wall material; High Z wall material

1. Introduction

For fusion devices in a divertor configuration, the selection of suitable divertor target materials is of crucial importance. The direct contact of the plasma with the target plates leads to material erosion, which in turn may result in contamination of the confined plasma with the respective impurities. Among the materials considered for target plate design, carbon and tungsten are presently considered most favorable, in particular because they are best suited to withstand a high stationary heat load as well as transient pulses.

However, both materials suffer from a number of disadvantages. While tungsten has a high sputtering threshold for deuterium, the tolerable concentration in the core plasma is on the other hand very small and sputtering could be enhanced by other impurities. Carbon is not as critical as tungsten with respect to the impurity concentration but even under low temperature, high density divertor conditions, there might be substantial carbon production due to chemical erosion. While the basic properties of plasma facing materials have been investigated to great detail in laboratory experiments and using computer simulations, the results obtained under such idealized conditions still need to be tested with results from experiments in the real environment. In the following, we present such results from erosion studies by analysis of material probes exposed to plasma discharges.

2. Experimental

For the investigation of erosion and deposition processes in the divertor of ASDEX Upgrade under realistic conditions, a manipulator probe system was constructed, which allows exposure of test tiles in the outer divertor plate for single discharges (Fig. 1). Up to six probes are held in a magazine where they are fetched by the manipulator and moved to a special purpose segment in the outer target plate. The probe takes the position of a removable tile, which is mounted on a pneumatically driven swivel arm mechanism. Probe exchange is possible between two subsequent discharges and an air lock system allows replacement of the magazine between discharges for ex-situ analysis of the probes.

Video observation of the probe surface and spectroscopic investigation of impurity fluxes above the probes is

* Corresponding author. Tel.: +49-89 3299 1655; fax: +49-89 3299 1149; e-mail: krieger@ipp-garching.mpg.de.

PII S0022-3115(96)00587-9

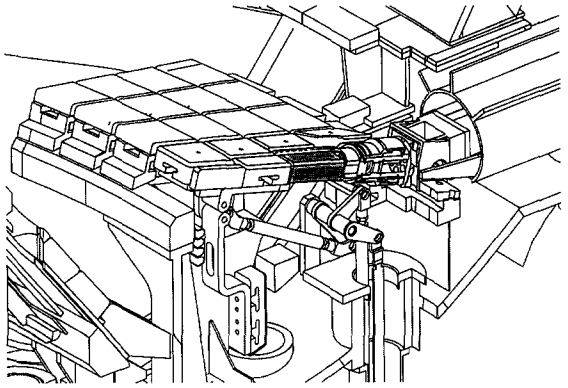

Fig. 1. Schematical view of the probe manipulator geometry at the outer target plate.

provided by the ASDEX Upgrade boundary layer spectrometer [1], which is equipped with a mirror system to allow observation of approximately two thirds of the AUG interior. The telescope optics of the spectrometer allows for a spatial resolution of < 5 mm at the target plates.

For the interpretation of the probe analysis results, the particle flux onto the target plates and the energy of the incident particles must be known. For interpretation of the spectroscopic observations, electron density n_e and temperature T_e above the target plates are required. Direct measurement of these quantities at the target plates is performed by a set of flush mounted Langmuir probes. To obtain information on the variation of n_e and T_e along the magnetic field lines in the divertor, radial profiles of both n_e and T_e are provided by a sweeping Langmuir probe system some centimeters above the outer target. The poor spatial resolution of the target Langmuir probes can be compensated by mapping the profile shape of the sweeping probe along the magnetic field lines down to the target and matching the absolute value to the target measurements.

To model the erosion processes with subsequent transport of impurities in the scrape-off layer and eventual redeposition, the trace impurity Monte-Carlo code DIVIMP [2] is used. The necessary plasma background model can be established by either using the internal DIVIMP 'onion skin' plasma model or results from the B2 code [3]. For iterative modelling of the neutral particle transport, EIRENE [4] is used in both cases.

Net erosion, i.e. the difference between erosion and subsequent redeposition, is determined by probes covered with thin layers of the respective material and measuring the thickness of the material before and after exposure in one or several subsequent discharges. The ion beam methods used for surface analysis also provide information on the depth distribution of the remaining material. In the case of carbon, the isotope ^{13}C was used for the probe preparation to distinguish between the probe material and the intrinsic carbon content of the machine. Deposition and implantation of impurities and deuterium from the discharge were analyzed by exposure of clean graphite probes and subsequent surface analysis.

For quantitative analysis of high Z material on the graphite substrate, Rutherford backscattering (RBS) with ^4He ions in the energy range from 0.7–2 MeV is used. This method also allows to distinguish the ^{13}C from the ^{12}C isotope. Implanted deuterium was detected using a ^3He ion beam and the nuclear reaction $^3He(D,p)\alpha$.

The contamination of tungsten with light impurities cannot be determined by RBS analysis. In this case, the surface was analyzed by Auger electron spectroscopy (AES) and X-ray photoelectron spectroscopy (XPS), which are sensitive to only the first few atom layers. In order to obtain depth distributions, the surface can be removed step by step using argon sputtering.

3. Carbon erosion studies

The erosion of carbon as target plate material in ASDEX Upgrade was investigated in Ohmic deuterium discharges at medium plasma density and in neutral beam heated L-mode discharges at high plasma density. Graphite test tiles with a 150 nm ^{13}C coating were used. Since the erosion was expected to be too small to obtain a significant effect in only one discharge, the probes were exposed to series of similar subsequent discharges. Fig. 2 shows the ^{13}C thickness obtained by RBS analysis before and after probe exposure in the L-mode discharges. The erosion is quite uniformly distributed along the radial target coordinate.

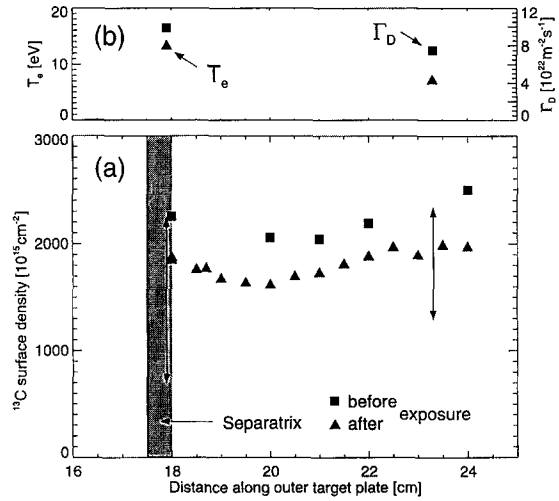

Fig. 2. (a) Thickness of ^{13}C layer before and after 4 s exposure to L-mode discharges ($\bar{n}_e = 6.3 \times 10^{19}$ m^{-3}, $P_{NBI} = 5$ MW) in radial direction along the target plate. The arrows denote erosion values as expected from ion beam experiments on physical sputtering and chemical erosion of carbon. (b) Results from flush mounted target Langmuir probes.

To determine erosion yields, we assume stationary plasma conditions. In that case, the surface density of the eroded material N_z, which is given by the difference of the measurements before and after exposure, can be expressed by

$$N_z = \int \Gamma_z \, dt = \int Y \Gamma_{D^+} \, dt = Y \Gamma_{D^+} \Delta t \quad (1)$$

where Γ_z is the net flux of eroded material atoms, Y is the erosion yield and Γ_{D^+} is the flux of incident plasma ions. For the determination of Γ_{D^+}, the inclination of the magnetic field lines to the target plates, θ, must be taken into account. Assuming sound speed

$$c_s = \sqrt{(3T_i + T_e)/m_i} \quad (2)$$

for the plasma particles entering the sheath [5] and $T_e \simeq T_i$ one obtains

$$\Gamma_{D^+} = n c_s \sin\theta \quad (3)$$

The erosion yield is then finally given by

$$Y = N_z / \left(n_e \sqrt{4T_e/m_i} \sin\theta \Delta t \right) \quad (4)$$

Using Eq. (4), one obtains in the vicinity of the strike point $Y_{eff} \simeq 1.2 \times 10^{-2}$ in the L-mode discharges and $Y_{eff} \simeq 0.5 \times 10^{-2}$ in the Ohmic discharges. Because the eroded ^{13}C isotope can be distinguished from redeposited ^{12}C from other locations, the measured yields can be attributed to gross erosion in this particular case. For comparison, the arrows in Fig. 2 denote the erosion for the L-mode scenario as expected from ion beam results on the erosion yield of physical and chemical sputtering. Despite uncertainties in the measurement of the particle flux and energy at the target, the measured target erosion is clearly smaller. However, the occurrence of chemical erosion is evident from other diagnostics, like mass spectrometry of the exhaust gas [6]. A possible explanation for this behavior, which is also observed in the Ohmic case, is a decrease of the chemical erosion with ion flux, as described in [7] by a factor of 3 to 5 respectively. Consequently, the observed hydrocarbons might be explained by production at the main vessel walls where the hydrogen flux is orders of magnitude smaller than at the divertor plates.

4. Tungsten erosion

In earlier tokamak experiments with tungsten limiters, the plasma contamination due to limiter erosion and close limiter-plasma contact reached intolerable levels. The usage of tungsten as target plate material appears much more favorable, in particular for reactor relevant high density low temperature divertor operation. To investigate the feasibility of tungsten in a divertor machine, ASDEX

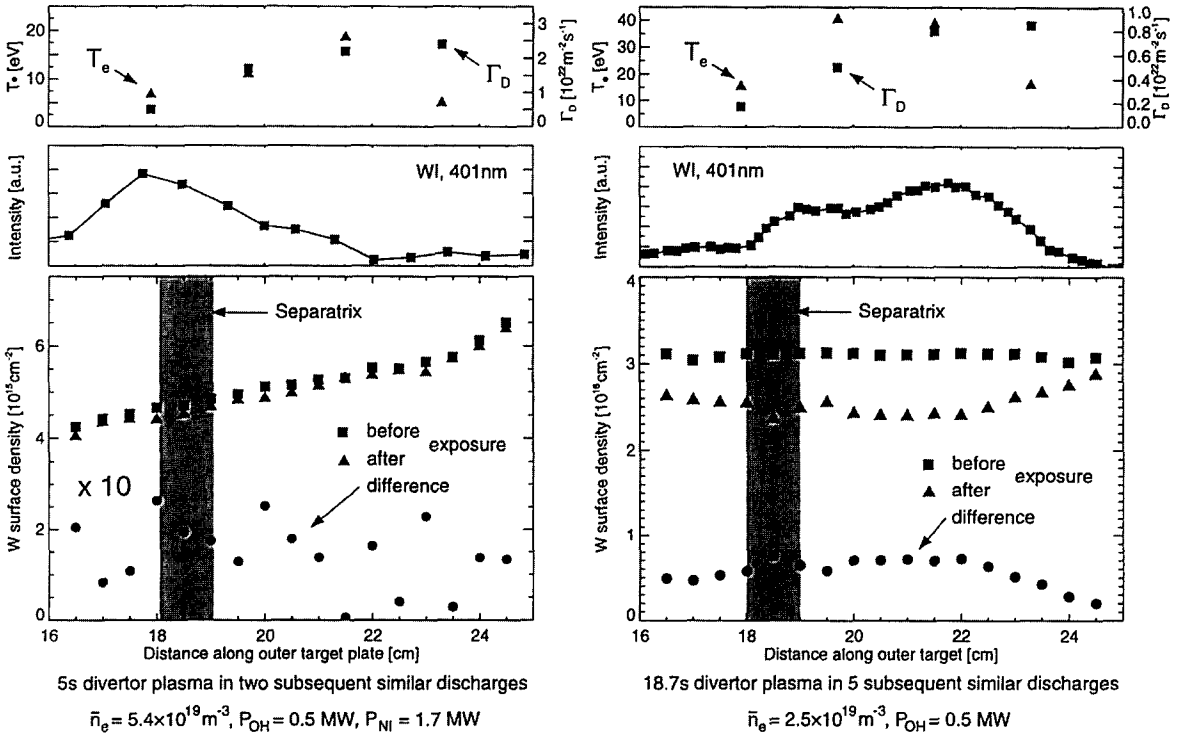

Fig. 3. Results from erosion measurements in L-mode (left) and Ohmic discharges (right) with spatial profiles of the WI spectral line emission above the target and T_e and Γ_D measurements from flush mounted target Langmuir probes.

Upgrade was equipped with tungsten coated graphite divertor tiles. Quantitative determination of tungsten erosion is not possible by spectroscopic measurements because tungsten atomic rate coefficients are very uncertain. As an alternative, probe measurements were done for Ohmic and NBI-heated L-mode discharges as well as for H-mode discharges.

For erosion measurements, tungsten marker stripes with a thickness of 1–20 nm were prepared on graphite probe tiles in radial direction using vapor deposition.

4.1. Ohmic and L-mode discharges

Fig. 3 shows the results for a probe exposed in medium density L-mode discharges and for a similar probe exposed in a series of low density Ohmic discharges. The L-mode case is an example of a divertor plasma with comparatively low temperature and high density. Consequently, the observed erosion is almost negligible, with an upper limit of $Y_{\mathrm{eff}} \simeq 1.5 \times 10^{-5}$, which is close at the detection limit. Similar values can be estimated from measurements of tungsten eroded at other divertor tiles and subsequently deposited on a pure graphite collector probe.

The Ohmic discharge series represents an operating regime with high temperature–low density conditions in the divertor. In this case, the observed effective tungsten erosion yield related to the incident D^+-flux reaches a value of $Y_{\mathrm{eff}} \simeq 5 \times 10^{-4}$ at the strike point. The spatial distribution of the WI spectral line emission is clearly correlated with the probe erosion pattern. Comparison of the line emission with results from material probe analysis and taking into account Langmuir probe temperature and density measurements could be used to obtain a rough absolute calibration of the WI line.

4.2. H-mode discharges

Comparison with the Langmuir probe data in the Ohmic and L-mode experiments showed that the tungsten erosion depends strongly on the plasma temperature. Therefore, substantial erosion by ELM temperature pulses was expected for H-mode discharges.

Surprisingly and in contrast to Ohmic and L-mode discharges where, except for erosion, no modification of the initial tungsten layer was found, in H-mode discharges the initial layer became distributed deeply into the graphite substrate material.

Fig. 4 shows the tungsten depth distribution in the vicinity of the strike point from RBS analysis of a 2 nm tungsten marker after exposure to a series of 5 MW neutral beam heated H-mode discharges. The deepest penetration of $\simeq 400$ nm is obtained at the position where the temperature reaches is maximum during an ELM heat pulse. Langmuir triple probes were used to measure the temporal evolution of the temperature on the ELM time scale. The peak value during ELM's reached 60 eV. This is, however,

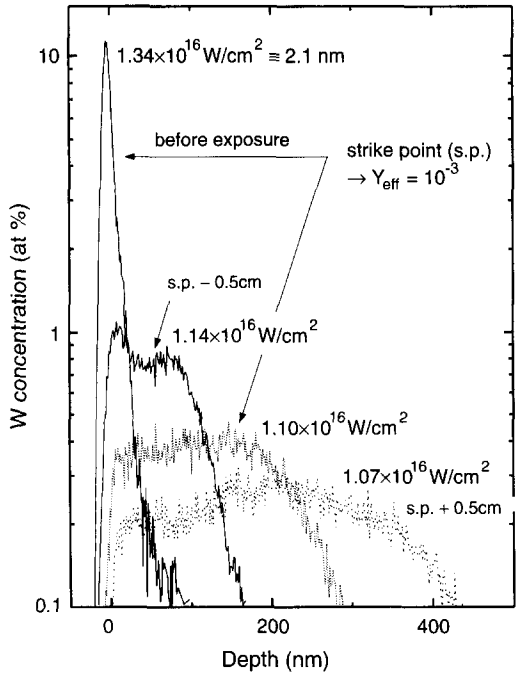

Fig. 4. Depth distribution of a tungsten marker at the separatrix strike point before and after exposure to a 5 MW H-mode discharge. The two curves denoted with s.p. − 0.5 cm and s.p. + 0.5 cm represent the depth distribution 0.5 cm inward and outward of the strike point location. The given tungsten surface densities are obtained by integrating over the respective depth profile.

a lower limit because the probes are restricted from measuring higher temperatures by their voltage supply. Simulations of ELM behavior with the B2/EIRENE code [8] result in higher temperatures up to 100 eV at the strike point.

Since the plasma temperature between ELM's is comparatively low ($\simeq$ 15–20 eV), one can attribute the observed effects to the ELM's alone. With an ELM frequency of 180 Hz and an ELM duration of $\simeq 0.5$ ms the resulting time integral over all ELM peaks is 0.5 s. By integrating over the depth distribution of the remaining tungsten and comparison with the initial thickness using Eq. (4), one obtains an erosion yield of 10^{-3}. This may be a lower limit as increasing W dilution in the surface layer will reduce subsequent W erosion.

4.3. Comparison with results from simulations

The impact energy of an ion incident on a material surface is given by it's thermal energy and by the energy gained in the sheath

$$E_{\mathrm{i}} = \tfrac{3}{2}kT_{\mathrm{i}} + \tfrac{1}{2}kT_{\mathrm{e}} + Z\gamma kT_{\mathrm{e}} \simeq (3Z+2)kT_{\mathrm{e}} \qquad (5)$$

for $\gamma = 3$ and $T_{\mathrm{e}} = T_{\mathrm{i}}$.

Fig. 5 shows a comparison of the measured effective erosion yields for the described scenarios with results from

TRIM sputtering simulations taking into account the energy and angular distribution of an isotropic Maxwellian distribution accelerated in the sheath potential [9]. In Ohmic and L-mode discharges the energy of the deuterium ions is too low to result in significant sputtering of tungsten, while it contributes to 50% in H-mode discharges. Carbon, which is still the main plasma impurity, is ionized in the charge state C^{4+} at these temperatures. The resulting impact energy $E_{C^{4+}} \simeq 14kT_e$ is sufficient to cause significant sputtering. However, the calculated effective sputtering yield for a carbon concentration of 1% is by a factor 5–10 higher than the measured values. A plausible explanation for this observation is the effect of prompt local redeposition of W^+ ions within their first gyro orbit after ionization, which occurs because of the small ratio of ionization length to gyro orbit radius of W^+ [10].

4.4. Long term effects on tungsten coating

In order to monitor the long term evolution of the built in tungsten coated target tiles, a probe with a similar plasma spray coating was exposed routinely to discharges. After 74 mainly Ohmic discharges, the probe was analyzed for implanted deuterium. The resulting radial profile of the deuterium surface density increases strongly towards the average position of the strike point.

The observed deuterium concentration is mainly attributed to codeposited carbon. The depth distribution of carbon in the tungsten coating was measured by stepwise erosion of the surface layer and analysis with Auger electron spectroscopy. Fig. 6 shows the results at the position of the highest D content. Near the surface, the tungsten fraction is only 40% and increasing to approximately 70% in a depth of 500 nm. In a depth of 40 nm a stoichiometry close to a tungsten carbide (W/C ≃ 1) is obtained, which can account for a high level of deuterium retention [11]. The broad distribution may be a result of the high surface roughness of the plasma spray coating. Therefore, pure tungsten may only be found in depths larger than the grain size > 10 μm. The results show that in a machine with carbon wall elements, it is impossible to maintain a divertor with clean tungsten target tiles. This will tend to reduce the tungsten erosion and increase the retained hydrogen isotopes and has to be taken into account in further studies of tungsten as divertor material.

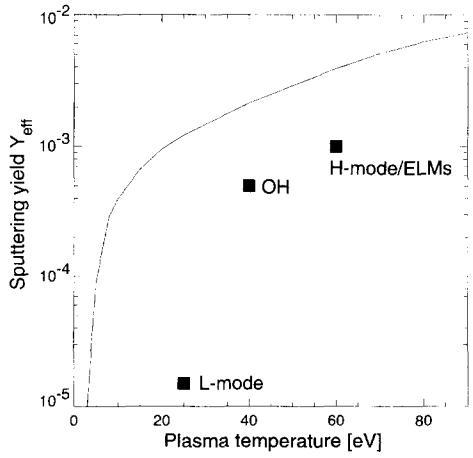

Fig. 5. Measured net erosion compared to results from ion beam experiments and TRIM simulations.

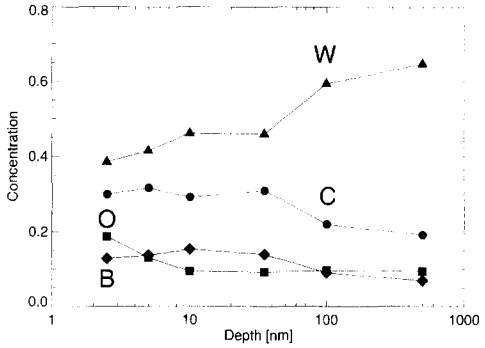

Fig. 6. Depth profiles of tungsten and light impurities near the average strike point position on a tungsten long term probe tile.

5. Summary

Erosion of carbon and tungsten in the divertor of ASDEX Upgrade has been studied by exposure of material probes in various discharge scenarios. The net erosion of thin layers of the respective material was determined by surface analysis using ion beam methods. Combining these results with measurements of plasma temperature and ion flux at the target by Langmuir probes, it was possible to determine erosion yields for different plasma conditions.

In the case of carbon, the resulting yields are higher than expected from physical sputtering by the incident plasma alone. Chemical erosion processes might account for the missing contributions. The measured erosion is, however, smaller than the chemical erosion yields as measured in low flux ion beam experiments. Decrease of chemical erosion with increasing flux has been observed in a number of other experiments and could explain the discrepancy.

The observed tungsten erosion yields are smaller than the theoretically expected values in the whole temperature range covered by these experiments. On the other hand, prompt local redeposition due to the small ratio of ionization length and W^+ gyro radius leads to an effective 80–90% decrease of the observed net erosion. Taking this in account, a much better agreement with erosion calculated from ion beam results is obtained.

Apart from erosion, further modifications of the originally clean tungsten surface were found. Carbon, which is

still used to cover most of the plasma facing wall elements and boron from the boronization procedure are intermixed quite deeply into the surface. The resulting modifications of the tungsten material properties have to be taken into account for the future use of tungsten in conjunction with carbon as plasma facing material.

References

[1] A.R. Field, J. Fink, D.R., G. Fussmann, U. Wenzel and U. Schumacher, Rev. Sci. Instrum. 66 (1995) 5433–5441.
[2] P.C. Stangeby, C. Farrell, S. Hoskins and L. Wood, Nucl. Fusion 28 (1988) 1945.
[3] B.J. Braams, A multi-fluid code for simulation of the edge plasma in tokamaks, Tech. Rep. EUR-FU/XII-80/87/68, NET Team (Garching, 1987).
[4] D. Reiter, Randschicht Konfiguration von Tokamaks, Entwicklung und Anwendung stochastischer Modelle zur Beschreibung des Neutralgastransports, Rep. Jül-1947, KFA Jülich (Germany, 1984).
[5] K. Riemann, J. Phys. D 24 (1991) 493.
[6] W. Poschenrieder, K. Behringer, H.S. Bosch, A.R. Field, C. Garçia-Rosales, A. Kallenbach, M. Kaufmann, J. Küppers, K. Krieger, G. Lieder, R. Neu, J. Neuhauser, D. Naujoks, J. Roth and the ASDEX Upgrade Team, J. Nucl. Mater. 220–222 (1995) 36–49.
[7] J. Roth and C. Garcia-Rosales, Analytic description of the chemical erosion of graphite by hydrogen ions, Nucl. Fusion (1997), in press.
[8] D. Coster et al., these Proceedings, p. 690.
[9] W. Eckstein, C. Garçia-Rosales, J. Roth and W. Ottenberger, Sputtering Data, Rep. IPP 8/82, Max-Planck-Institut für Plasmaphysik (Garching, 1993).
[10] D. Naujoks, K. Asmussen, M. Bessenrodt-Weberpals, S. Deschka, R. Dux, W. Engelhardt, A. Field, G. Fussmann, J. Fuchs, C. Garcia-Rosales, S. Hirsch, P. Ignacz, G. Lieder, F. Mast, R. Neu, R. Radtke, J. Roth, U. Wenzel and ASDEX Upgrade Team, Nucl. Fusion 36 (1996) 671.
[11] W. Wang, V. Alimov, B. Scherzer and J. Roth, these Proceedings, p. 1087.